The interface between benzenes (C_6H_6;C_6H_5Cl;2-C_6H_4OHCl) and amorphous solid water studied with metastable impact electron spectroscopy and ultraviolet photoelectron spectroscopy (HeI and II)

A. Borodin, O. Höfft, U. Kahnert, and V. Kempter[a)]
Institut für Physik und Physikalische Technologien der Technischen Universität Clausthal, Leibnizstr. 4, D-38678 Clausthal-Zellerfeld, Germany

S. Krischok
Institut für Physik und Zentrum für Mikro- und Nanotechnologien der TU Ilmenau P.O. Box 100565, D-98684 Ilmenau, Germany

M. O. Abou-Helal
Natl. Res. Center, Sol. State Phys. Dept., El-Tahrir St., Dokki, Cairo, Egypt

(Received 8 October 2003; accepted 19 December 2003)

Interfaces between films of benzenes (C_6H_6;C_6H_5Cl;2-C_6H_4OHCl) and solid H_2O on tungsten substrates were studied between 80 and 200 K with metastable impact electron spectroscopy (MIES) and ultraviolet photoelectron spectroscopy [UPS(HeI and II)]. The following cases were studied in detail: (i) Adsorption of the benzenes on solid water in order to simulate their interaction with ice particles, and (ii) deposition of water on benzene films in order to simulate the process of water precipitation. In all cases the prepared interfacial layers were annealed up to 200 K under *in situ* control of MIES and UPS. The different behavior of the interfaces for the three studied cases is traced back to the different mobilities of the molecules with respect to that of water. The interaction between H_2O and the benzenes at the interfaces is discussed on the basis of a qualitative profile for the free energy of that component of the interface which has the larger mobility. Possible implications of the present results for atmospheric physics are briefly mentioned. [DOI: 10.1063/1.1648018]

I. INTRODUCTION

The chemistry on molecular films, water in particular, is a challenging field for surface science because of the complexity of the three-dimensional system under study. The chemistry occurs here in a highly dynamic, quasi-liquid molecular environment where the balance between solvation, chemical reactions, stabilization of the solute and the reaction products are important factors.[1–5] In fact, the ice–frozen water interface is constantly changing as water molecules adsorb and desorb. Adsorbing species may become solvated quickly and encapsulated into a water matrix.[6,7]

Persistent, bioaccumulative, and toxic substances (PBT's) are of global and local concern: Photochemical reactions involving PBT's play a mayor role in the atmosphere, in natural water, on soil, and in living organisms.[8] Snow and ice are important components of cold ecosystems and influence the fate and the reactions of PBT's. The process of uptake of these chemicals into nascent water crystals can take place either by adsorption onto the surface of precipitating snow crystals or through co-deposition with water into growing crystals or films.

Our present understanding of how PBT's interact with frozen water is relatively limited, and the study of the interaction has only recently become a subject of detailed investigations. A quantitative model to assess and evaluate the environmental fate and behavior of PBT's in cold ecosystems would include to know about:[8]

(i) the efficiency and the mechanism of snow scavenging from the atmosphere by the chemicals;
(ii) the behavior (migration, solvation, etc.) of the chemicals within snow or ice particles; and
(iii) the release, i.e., the desorption of chemicals, products from photochemical reactions in particular, into the ecosystem.

The photolysis of the substances in ice yielded photoproducts very different from those observed in liquid water:[8] The observed preferential formation of dimers of the starting molecules gives evidence for their high concentration in the reaction region. This was explained in terms of an effective reaction cavity which restricted the reactions between the host water molecules and the guest organic substances. In order to shed more light into the origin of the different photochemistry of PBT's in solid and liquid water, we have applied the ultra-surface sensitive metastable impact electron spectroscopy (MIES), in combination with photoelectron spectroscopy (UPS with HeI and II), to the study of interfaces between the benzenes C_6H_6, C_6H_5Cl, and 2- (or ortho-) C_6H_4OHCl and solid water between 80 and 200 K. In contrast to C_6H_6 and C_6H_5Cl, 2-C_6H_4OHCl may interact with water comparatively strongly via its OH-group. In order

[a)]Telephone: +49-5323-72-2363; Fax: -72-3600. Electronic mail: volker.kempter@tu-clausthal.de

to obtain information on the PBT–water interaction under atmospheric conditions, we studied (i) the adsorption of the benzenes on solid water, simulating the interaction of the chemicals with ice and snow particles, and (ii) the deposition of water on films of the benzenes, simulating the process of water precipitation. (ii) may also provide a better understanding of the interaction of water with soot particles in aircraft contrails:[9] The films of organic rings serve as a model for the soot particle's surface while the ligands form functional groups for the interaction with water molecules.

II. EXPERIMENT

The experiments were carried out under ultra high vacuum (UHV) conditions (base pressure $<4\times10^{-10}$ Torr) equipped with low energy electron diffraction (LEED), x-ray and ultraviolet photoelectron spectroscopy (XPS and UPS) (HeI and II), Auger electron spectroscopy (AES), and MIES, and are described in detail elsewhere.[10,11] In MIES metastable helium atoms ($2\,^3S/2\,^1S$) of thermal kinetic energy are utilized to eject electrons from the uppermost layer of the surface. The application of MIES to surface spectroscopy is well documented.[4,12] Previous applications of MIES, in combination with UPS, to the characterization of films of solid water and to the study of processes taking place on these films as a consequence of the adsorption of atoms and molecules can be found elsewhere.[5,13–16]

The energy scales in the figures are adjusted in such a way that electrons emitted from the Fermi level, i.e., electrons with the maximal kinetic energy, appear at the binding energy $E_B=0$ eV. The position of the Fermi level is determined from MIES spectra for Na-covered tungsten.[14,17] In the following, all binding energies refer to the Fermi level ($E_B=0$ eV). The low-energy cutoff in the spectra gives directly the surface work function, irrespective of the actual interaction process which produces the electrons.

The employed benzenes were dosed to the surface by backfilling the chamber with the desired molecules at a pressure of about $2\cdot10^{-8}$ Torr. The procedure for obtaining an estimate of the molecular coverage is discussed in more detail in Ref. 15. Briefly, we benefit from the fact that the MIES signal saturates after completion of the first molecular adlayer, and that in UPS(HeI) the emission at the Fermi level disappears roughly at a coverage of two complete adlayers for the chemicals under consideration. The exposure is given in units of monolayer equivalents (MLE). At 1 MLE the surface would be covered by one molecular adlayer; penetration of the molecules into the host solvent film may, however, modify the coverage. The amount of surface-adsorbed water can be estimated on the basis of earlier work with TPD and MIES.[11,13] The surface temperature can be varied between 80 and 700 K; the absolute value of the temperature is known within $+/-10$ K. The surface was exposed to water by backfilling the chamber at a substrate temperature between 110 and 130 K. This ensures the formation of a dense, nonporous and amorphous film of solid water.[18] The formation of an ordered film would require a certain degree of mobility of the water molecules; below 140 K this mobility does not exist anymore. No extra spots were observed with LEED when dosing the tungsten substrate with water; no substrate spots are seen anymore when the coverage exceeds 5 MLE.

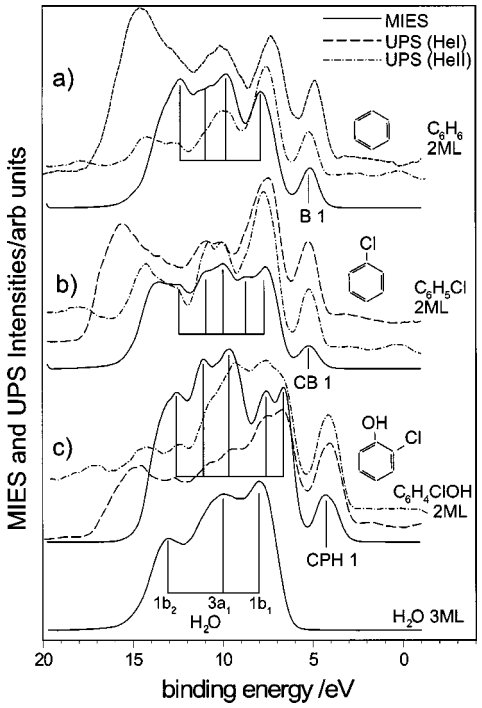

FIG. 1. (a) MIES spectra for the adsorption of water on tungsten (80 K), and MIES and UPS(HeI and II) spectra for benzene (B) (2ML) on water films (80 K; 3BL). See text for the identification of the structures labeled by vertical bars. (b) As Fig. (a), but for chlorobenzene (CB). (c) As Fig. (a), but for chlorphenol (CPH).

III. RESULTS

Figures 1(a)–1(c) compare MIES and UPS(HeI and II) spectra for benzene (B) [Fig. 1(a)], chlorobenzene (CB) [Fig. 1(b)], and 2-chlorophenol (CPH) deposited on a solid water film supported by a tungsten substrate. Also shown are MIES spectra for water adsorbed on tungsten; UPS data for water can be found elsewhere.[5,11,19,20] Water, when adsorbed molecularly, produces three peaks identified as emission from the three uppermost occupied water orbitals $1b_1$, $3a_1$, and $1b_2$[19,20] ($E_B=7.8$; 10.0; 13.2 eV, respect.). In contrast, the adsorption of water onto partially alkalated titania, leading to water dissociation, yields peaks at $E_B=7.0$ and 11.2 eV from the ionization of the OH 1π and the 3σ orbitals, respectively.[19,20] In the present work we see only the emission from molecular water. The emission from $3a_1$ is comparatively broad and, apparently, reflects contributions to this molecular orbital (MO) from intra-molecular mixing, i.e., this MO consists of contributions from the wave functions of adjacent water molecules that interact via hydrogen bonding.[21]

The B spectra display 5 spectral features in MIES, B1 to B5, at $E_B=5.1$; 7.9; 9.8; 11.0; 12.4 eV, respect. [Fig. 1(a), see vertical bars]. They are due to the ionization of the benzene MO's $1e_{1g}(\pi_3/\pi_2)(B1)$, $1a_{2u}(\pi_1)/3e_{2g}(\sigma)(B2)$, $1b_{2u}(\sigma)/3e_{1u}(\sigma)(B3)$, $2b_{1u}(\sigma)(B4)$ and $3a_{1g}(\sigma)(B5)$.[22] It is of considerable importance for the data reduction lead-

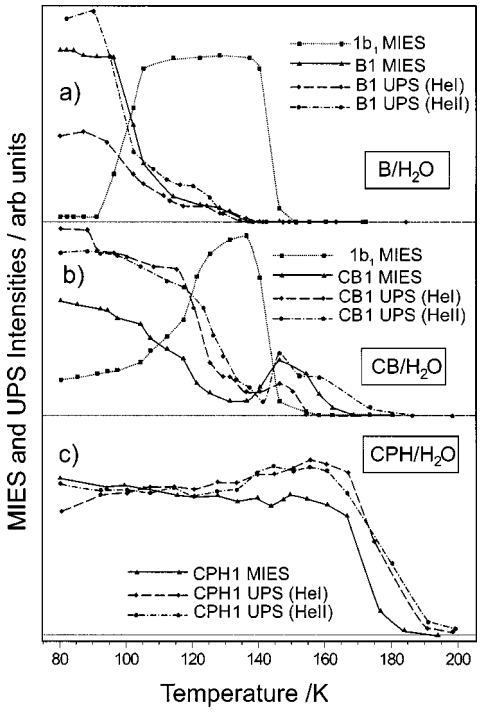

FIG. 2. (a)–(c) Intensity changes of various spectral features [$H_2O(1b_1)$ in MIES; B1 (CB1; CPH1) in MIES, HeI, and II] during the annealing of a film of benzene (1 ML) (a), chlorobenzene (1 ML) (b), and 2-chlorophenol (3 ML) (c) deposited on a water film (80 K; 3BL).

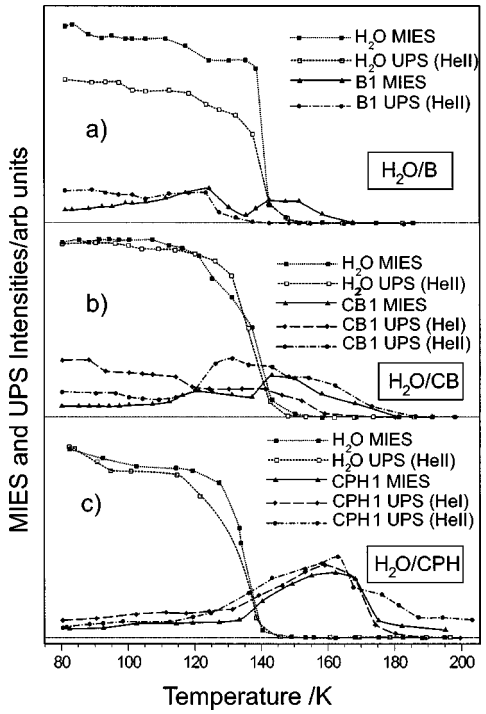

FIG. 3. (a)–(c) Intensity change of the MIES signals B1 (CB1; CPH1) and $H_2O(1b_1)$ during annealing a water film (2BL) deposited on films (about 3 ML thick) of benzene (a), chlorobenzene (b), and 2-chlorophenol (c) (80 K).

ing to the graphs of Figs. 2 and 3, that no contribution from the ionization of water interfers with $B1$. The peaklike emission seen at the largest binding energies in MIES and UPS (HeI) is due to secondary and/or scattered electrons with small kinetic energies.

The CB spectra display 6 features, CB1–CB6, at $E_B = 5.1$; 7.3; 8.8; 9.9; 10.9; 12.4 eV [Fig. 1(b), see arrows]. Penning ionization of C_6H_5X (X=F,Cl,Br,I) molecules in the gas phase upon collisions with metastable He atoms was studied by Penning ionization electron spectroscopy (PIES).[23] According to that work the following assignment can be given to the spectral features: $4b_1(\pi_3)/1a_2(\pi_2)$ (CB1), $9b_2(n_\perp)/3b_1(n_\parallel)$ (CB2), $2b_1(\pi_1)$ (CB3), $14a_1/7b_2$ (CB4), $6b_2/13a_1$ (CB5), and $12a_1$ (CB6). Again, as for B, the emission from the ionization of the lowest π MO's is well separated from any water emission, in particular from $1b_1$. CB2 stems from those MO's that are most strongly affected by an admixture of states with Cl3p character.[23]

The CPH spectra display 6 features, CPH1 to CPH6, at $E_B = 4.3$; 6.8; 7.6; 9.9; 11.0; 12.5 eV [Fig. 1(c), see bars]. On the basis of molecular structure calculations the following MO's can be expected to contribute strongly to the observed spectral features:[24] π_3/π_2 (CPH1), $n_\perp$(Cl)/$n_\parallel$(Cl) (CPH2), $n_\perp$(O)/π_{CCl} (CPH3), π_1 (CPH4), σ_{CC}/σ_{CO} (CPH5), σ_{CC}/σ_{CH} (CPH6). CPH1 is again well separated from any water emission.

All labeled features are seen both in the MIES, HeI, and II spectra. We have not made any attempt to identify additional feature seen at larger binding energies with HeII. This suggests that the MIES spectra are due to the Auger deexcitation process in which one electron from water or benzene valence band states fills the 1sHe vacancy while the 2sHe takes over the excess energy and is ejected in the Auger process.[4,12] However, the relative intensities in MIES and UPS spectra may differ:[4,12] In MIES the spectra reflect the density of the respective molecular states prior to ionization by Auger deexcitation, while the UPS spectra depend upon the density of states of both the initial and final states involved in the photoionization process, and thus on the so-called joint density of states. Furthermore, we can expect that those MO's that extend outside the repulsive molecular surface, as estimated from the van der Waals radii of the atoms in the molecule, give strong contributions to the MIES spectra.[23] For this reason π-bands will manifest themselves strongly in MIES in accordance with other conjugated molecules. Furthermore, n-bands should appear enhanced in MIES because, having Cl3p and O2p character, they will contribute strongly to the charge density that extends outside the repulsive molecular surface, and, thus, are not efficiently shielded by the charge density of the benzene ring. The same arguments apply to the MO's that form σ_{CCl}, σ_{CO} bonds.

Figures 2(a)–2(c) show the temperature dependence of the $1b_1$ and B1 (CB1; CPH1)-intensities in the MIES and UPS spectra for monolayers of benzenes deposited on solid water films. Figure 2(a) shows the results for benzene (B) (denoted by B–H_2O) as a function of the annealing temperature. At first, B is adsorbed atop. The simultaneous decrease of B1 in MIES and UPS seen above 95 K suggests that B starts to desorb from the water film, and has practically disappeared at 130 K. If B would penetrate into the water film, B1 should disappear in MIES, but would still be present in the UPS spectra which is not the case. With the onset of B

desorption $1b_1$ starts to rise because the shielding of water by B against the interaction with He* becomes less efficient. Around 140 K water starts to desorb, and, according to MIES and UPS, desorption is complete around 150 K.

Figure 2(b) presents the corresponding results for chlorobenzene (CB) deposited on solid water (denoted by CB–H_2O). The simultaneous decrease of CB1 in MIES and UPS and the rise of $1b_1$ seen between 115 and 140 K indicate that the desorption of CB species becomes sizeable above 115 K. However, although CB1 has become rather small around 135 K in MIES, desorption is not complete at that point because CB reappears both in MIES and UPS at $T>140$ K during water desorption. The small CB1 signal between 120 and 140 K suggests, in particular, that CB is shielded from the interaction with He*, and, consequently, implies that in this temperature range the toplayer consists of water mainly. The CB species that are bound to the tungsten substrate are seen up to 165 K.

Figure 2(c) displays the corresponding results for a 2-chlorophenol (CPH) film (denoted by CPH–H_2O). CPH covers the water film as signaled by the absence of water-induced features in both MIES and UPS. No significant change of the CPH1 intensity has yet occurred at 150 K where water should have desorbed to a large extent; CPH desorption becomes significant above 170 K. No water-induced emission is seen in the entire studied range of temperatures. Apparently, the high temperature for CPH desorption originates from an increased interaction among the CPH molecules, probably caused by H-bonding, involving the OH-group of CPH.

Figures 3(a)–3(c) show the temperature dependence of the $1b_1$ and $B1$ (CB1; CPH1)-intensities in the MIES and UPS spectra when water overlayers deposited on films of the benzenes are heated between 80 and 200 K. In all cases water desorption takes place at about the same temperature (around 140 K); no significant influence of the ligands can be noticed. In particular, no indication of an eventual H-bonding is apparent for CPH. Figure 3(a) shows the results for a water overlayer (2BL) on benzene (B) (denoted by H_2O–B). Initially, water forms the top layer as judged from the fact that only very weak B1 emission, besides the spectral features from molecular water, can be noticed, i.e., efficient shielding of B by the water molecules takes place. The rise of B1 in MIES, noticeable already below 100 K, cannot simply be attributed to water desorption. Considering the absolute surface sensitivity of MIES, we conclude that some B species have moved closer to the surface of the water film, and, to some extent, become accessible to MIES. A second maximum in the B1 signal occurs when most of the water has desorbed, i.e., around 150 K, and the remaining B species are not shielded anymore efficiently. The B species responsible for this rise are directly bound to the tungsten substrate as is also suggested by the fact that the position of B1 is shifted by 0.5 eV towards smaller binding energies. The comparison with the spectra collected during the deposition of B (before offering water) indicates that at 145 K the B coverage of the substrate is only of the order of 20 percent [too low to be detected with HeII]. B desorption is impeded by about 15 K as compared to B–H_2O when the B layer is water-covered.

Figure 3(b) shows the corresponding results for H_2O–CB; parameters are as given in Fig. 3(a). At a first glance, the results appear to be qualitatively similar as for B. However, the decrease of $H_2O(1b_1)$ is more gradual and sets in earlier (around 120 K, instead of 137 K for B); the CB1 emission seen after water desorption (at 150 K) is still about 50 percent of that before exposure of the CB film to water. Not before 190 K all CB species have desorbed from the tungsten substrate.

The results for H_2O–CPH [Fig. 3(c)] are qualitatively different: CPH1 rises in MIES and UPS as soon as the shielding of CPH by water molecules becomes reduced, i.e., beyond 130 K. At 160 K the entire amount of CPH deposited prior to water exposure is still present.

For the following discussion we note from Figs. 2 and 3 that desorption from tungsten takes place between $T_D=160$ and 190 K for all studied benzenes. On the other hand, desorption from water occurs earlier, at $T_D=110$ and 130 K for B and CB, respectively. Here T_D denotes the temperature at which the intensities of B1 and CB1 have decayed to $1/e$. For H_2O–CPH multilayers are still stable on tungsten after the water has desorbed; for H_2O–B and –CB part of the underlying B and CB films has desorbed together with the water.

IV. DISCUSSION

The interaction of an adsorbate, in particular its penetration into the solvent, is often discussed in terms of the free energy (FE) behavior of the adsorbate as a function of its distance from the solvent surface.[2,25] As discussed in more detail in Ref. 2, the FE-profile can be expressed as the sum of the average kinetic and potential energies and an entropy term, related to the disorder caused by the presence of the adsorbate. When the adsorbate approaches the surface, the potential energy term decreases monotonously, and reaches a minimum close to the surface. This is due to the increasing coordination number of the water molecules surrounding the adsorbate and/or to (hydrogen) bond formation. Qualitatively, the entropic contribution follows the behavior of the potential energy, indicating an entropy loss caused by the increase of order when the adsorbate, entering the surface, becomes trapped by solvent molecules. Inside the solvent, the profile depends on subtle changes in the potential energy and the entropy of the system, and, thus, on the solvation ability of the solvent, i.e., on the type of the adsorbate–solvent interaction.

For B–H_2O water will be considered as the solvent because B desorbs from water at 105 K while a water film on tungsten is stable up to about 140 K. The interaction at the (H_2O–B)-interface will be discussed with the help of Fig. 4(a). It presents, qualitatively, the FE profile of a B molecule as a function of its distance z from the water surface. Minimum (I) (depth V_{SG}) is responsible for the on-top adsorption at 80 K. The rise of FE during the penetration of B into the solvent ($z<0$) reflects the fact that no bond formation nor an appreciable energy gain from an increase of the coordination number of the water molecules takes place under these circumstances. Instead, the large value of V_{SB} is attributable to the geometric reason that for penetration the large B mol-

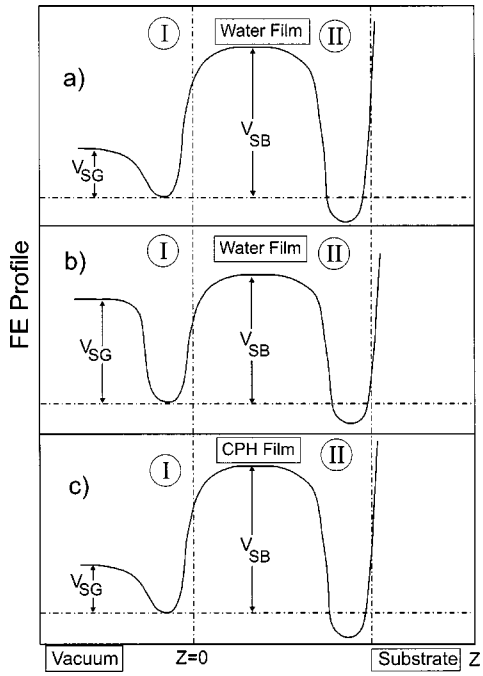

FIG. 4. (a)–(c) Free energy profiles (qualitatively) for the interaction at interfaces between water and the benzenes (a) C_6H_6, (b) C_6H_5Cl, and (c) 2-C_6H_4OHCl. V_{SG} and V_{SB} are the barrier heights for desorption into the vacuum and migration into the solvent film, respectively; $z=0$ is at the interface between film and vacuum.

ecule need to push-out water molecules from their lattice sites. V_{SB} is a function of temperature, and will decrease with increasing water mobility. Another well (II) [Fig. 4(a)] is noticed at the H_2O–substrate interface. This stable site for B adsorption arises from the B–substrate interaction which, in general, can be stronger than the water–water or water–B interaction.

The observed temperature dependence of B1 and $1b_1$ simply implies that $V_{SG} \ll V_{SB}$; as explained above, the large B species are unable to enter the rather dense water lattice at temperatures much below T_D of water. As soon as the temperature becomes larger than T_D(B), the probability for B desorption from well (I) into the vacuum becomes rather high while that for migration into the film and to the tungsten substrate remains low. Consequently, B desorption causes the strong decrease of B1, seen both with MIES and HeII above 105 K, connected with the strong rise of $1b_1$. Clearly, all B species have desorbed before water desorption becomes significant.

For H_2O–B the B species are located in (II) initially [see results of Fig. 3(a)]. Figure 2(a) suggests that between 80 and 120 K the penetration of these B species into the water film is unlikely because of the large barrier V_{SB}. We have to explain the findings that, on the one hand, only about 20 percent of the originally deposited B species are present when all water has desorbed, and, on the other hand, only a weak B1 signal is observed in MIES at any temperatures. Obviously, the mobility of the water molecules has increased drastically at 130 K because of the shorter lifetime of the H-bonds. Thus, their larger mobility allows the water molecules to ''uncover'' the B species which, as a consequence, can desorb even though they were initially located underneath the water film. However, desorption is delayed as compared to B–H_2O (115 K). By applying TPD, it was demonstrated for CCl_4 and CD_3Cl that desorption is indeed impeded by an overlayer of solid water.[26,27] The probability for detecting B species at the surface for temperatures close to $T_D(H_2O)$ is, however, small: their residence time in (I) is short for T far above T_D(B), probably between 10^{-12} and 10^{-9} s,[2] because V_{SG} is small, and instantaneous desorption occurs into the vacuum. The onset of the water desorption above 135 K causes a rise of B1: those B species, still located in well (II), become now accessible to MIES. Indeed, we find that $T>165$ K is required to completely remove the B species deposited at 80 K on the tungsten substrate.

For the discussion of the interaction at the (H_2O–CPH)-interface we interchange the role of solvent and solute, treating CPH as solvent. This makes sense because T_D for H_2O on CPH is about 135 K, and CPH films are still stable on tungsten at this temperature. We arrive at the FE profile displayed in Fig. 4(c). (I) allows for on-top water adsorption of water, as observed for 80 K. For H_2O–CPH, water desorption becomes significant as soon as V_{SG} can be surpassed ($T>130$ K). Caused by the water desorption, CPH becomes accessible to MIES; this explains the correlation between the decrease of $1b_1$ and the rise of CPH1 [see Fig. 3(c)]. Other than for B–H_2O, we have assumed that the barrier V_{SB} is low because the water molecules can move relatively freely through the comparatively open CPH lattice. Thus, for CPH–H_2O, water molecules will migrate from II to I through the CPH lattice, as soon as water becomes mobile. Because V_{SG} is also low, the residence time of water species that have migrated through the CPH film to the surface is short (between 10^{-12} and 10^{-9} s),[2] and accounts for the absence of water-induced features in the spectra. By applying TPD it should be possible to verify at which temperature water desorption takes place for CPH–H_2O.

For the (CB–H_2O)-system both components become mobile at about the same temperature. Consequently, interpenetration of the two components takes place before desorption is complete. This is underlined by the fact that CB species, originally deposited atop of the water film, are found on the tungsten substrate after all water has desorbed. In the FE profile for (CB–H_2O) [Fig. 4(b)] the choice $V_{SG} \approx V_{SB}$ allows for the simultaneous occurrence of desorption and penetration.

By applying TPD, it was demonstrated for CCl_4 and CD_3Cl that desorption is impeded by an overlayer of solid water.[26,27] It was claimed that the formation of cages of the coadsorbates under water takes place on metallic surfaces.[26] No indication of caging is seen for the large organic molecules under study. For CCl_4 the desorption from underneath a water layer is correlated with the onset of water crystallization.[27] In concert with crystallization, the underlaying CCl_4 desorbs abruptly over a narrow temperature range. It was proposed that structural changes during crystallization may facilitate desorption pathways in the water overlayer. These pathways may arise from the formation of grain boundaries, cracks, and fissures, occurring during crystalliza-

tion. This mechanism may contribute to the observed B desorption through water.

The conclusions of this paper can be generalized to other substrates as well because the temperature for film formation, both of water and the benzenes, will show little dependence on the actual substrate.[19,20] Only the monolayer fraction that can be obtained above the temperature for desorption of the films does depend on the number and type of centers actively interacting with the benzenes. The density of active centers on substrates of interest for application, as functional groups on soot and point defects on oxides, will certainly be higher than on metals.

Finally, we make an attempt to apply our results to interfaces between benzenes and water under atmospheric conditions, say at 220–250 K:

(1) Exposure of the films of benzenes to water (precipitation of water on polluted surfaces): Prior to water exposure, T is larger than the temperature for desorption from the substrate on which the benzenes are deposited. Consequently, films of the benzenzes cannot form; only molecules borided sufficiently strongly to the substrate in well (II), in particular at substrate imperfections, are present. Following water exposure, there is little tendency of these, comparatively strongly bound molecules to migrate into the water toplayer. Therefore, under the conditions of (1), the benzenes will be found at the interface between the substrate and the water film.

(2) Benzenes inside ice particles: Due to the low solubility of benzenes in water, their frozen solution may be visualized as an ensemble of molecular agglomerates, embedded into ice cavities.[28] As suggested from the behavior observed for water deposited underneath CPH, water molecules from the surrounding cavity walls can be expected to pass freely through the relatively open agglomerate structure of the organic species. However, these species, although being mobile themselves, will not be able to enter the cavity walls to a large extent because of kinematic constraints (see Fig. 4). Consequently, their motion, at high concentration, remains largely restricted to the volume of the cavities; the water concentration inside the cavities will greatly depend on temperature.

When ice particles are exposed to benzenes, a similar argumentation shows that the organic species will accumulate at the outside of the particles, embedded into the aqueous atmosphere above the particle surface. Thus, a high concentration of the solute species is possible at the water–benzenes interface; indeed, this was concluded from the high probability for dimer formation in photoreactions of CPH with ice.[28]

V. SUMMARY

The interaction of the benzenes C_6H_6, C_6H_5Cl, and $2\text{-}C_6H_4OHCl$ with solid H_2O, deposited on tungsten, was studied with metastable impact electron spectroscopy (MIES) and ultraviolet photoemission spectroscopy (UPS) with He (I and II). The conditions were (i) adsorption of the benzenes on solid water in order to simulate the interaction of the chemicals with ice particles, and (ii) deposition of water on the organic films in order to simulate the process of water precipitation. In all cases, we studied the properties of the adsorbed layers during their annealing between 80 and 200 K. At 80 K, closed layers of all studied benzenes can be prepared on water with little mixing and *vice versa*.

For C_6H_6 on water ($B–H_2O$), desorption starts around 105 K; no penetration of B into the water film could be detected. For $H_2O–B$, B desorption appears to be delayed and starts when the water molecules of the overlayer become sufficiently mobile ($T>120$ K). B desorption is complete when the B molecules interacting comparatively strongly with the tungsten substrate have desorbed ($T=160$ K). For chlorobenzene on water ($CB–H_2O$), CB and water molecules both become mobile around 120 K and desorb in the same temperature range. Not all CB molecules desorb with the water film; some CB molecules interact with the tungsten substrate, and finally desorb at 170 K. For 2-chlorophenol on water ($CPH–H_2O$), all water has desorbed before CPH desorption sets in ($T=170$ K). We suggest that, as soon as the H_2O molecules of the underlayer become sufficiently mobile, e.g., above 120 K, water can migrate through the comparatively open CPH lattice. For $H_2O–CPH$ water has desorbed before any desorption of CPH can be detected (around 170 K).

Qualitative free energy profiles are proposed that can account for the experimental results. We predict that under atmospheric conditions the studied benzene species, when deposited on solid substrates, remain located at the interface under water exposure. On the other hand, benzenes will accumulate at the outside of benzenes-exposed ice particles. As solutes they remain aggregated in ice cavities of frozen solutions.

ACKNOWLEDGMENT

We thank P. Klan (Masaryk University, Brno) who suggested this work.

[1] G. E. Brown *et al.*, Chem. Rev. **99**, 77 (1999).
[2] C. Girardet and C. Toubin, Surf. Sci. Rep. **44**, 159 (2001).
[3] M. Faubel, in *Photoionization and Photodetachment, Part 1*, edited by C. Y. Ng (World Scientific, Singapore, 2000), p. 634.
[4] H. Morgner, Adv. At., Mol., Opt. Phys. **42**, 387 (2000).
[5] J. Günster, S. Krischok, V. Kempter, J. Stultz, and D. W. Goodman, Surf. Rev. Lett. **9**, 1511 (2002).
[6] D. R. Haynes, N. J. Tro, and S. M. George, J. Phys. Chem. **96**, 8502 (1992).
[7] L. Chaix, H. van den Bergh, and M. J. Rossi, J. Phys. Chem. A **102**, 10300 (1998).
[8] P. Klan and I. Holoubek, Chemosphere **46**, 1201 (2002).
[9] D. Ferry, J. Suzanne, S. Nitsche, O. B. Popovitcheva, and N. K. Shonija, J. Geophys. Res., [Atmos.] **107**, 4734 (2002).
[10] P. Stracke, S. Krischok, and V. Kempter, Surf. Sci. **473**, 86 (2001).
[11] S. Krischok, O. Höfft, J. Günster, J. Stultz, D. W. Goodman, and V. Kempter, Surf. Sci. **495**, 211 (2001).
[12] Y. Harada, S. Masuda, and H. Osaki, Chem. Rev. **97**, 1897 (1997).
[13] J. Günster, S. Krischok, J. Stultz, and D. W. Goodman, J. Phys. Chem. B **104**, 7977 (2000).
[14] S. Krischok, O. Höfft, J. Günster, R. Souda, and V. Kempter, Nucl. Instrum. Methods Phys. Res. **203**, 124 (2003).
[15] A. Borodin, O. Höfft, S. Krischok, and V. Kempter, Nucl. Instrum. Methods Phys. Res. **203**, 205 (2003).
[16] S. Krischok, O. Höfft, and V. Kempter, Surf. Sci. **532**, 370 (2003).
[17] M. Brause, S. Skordas, and V. Kempter, Surf. Sci. **445**, 224 (2000).
[18] K. P. Stevenson, G. A. Kimmel, Z. Dohnalek, R. S. Smith, and B. D. Kay, Science **283**, 1505 (1999).
[19] P. A. Thiel and T. E. Madey, Surf. Sci. Rep. **7**, 211 (1987).

[20] M. A. Henderson, Surf. Sci. Rep. **285**, 1 (2002).
[21] S. Casassa, P. Ugliengo, and C. Pisani, J. Chem. Phys. **106**, 8030 (1997).
[22] K. Kimura *et al.*, *Handbook of HeI Photoelectron Spectra of Fundamental Organic Molecules* (Halsted Press, N.Y., 1981).
[23] K. Imura, N. Kishimoto, and K. Ohno, J. Phys. Chem. A **105**, 4189 (2001).
[24] K. Ohno, private communication (2003).
[25] H. Shinto, T. Sakakibara, and K. Higashitani, J. Chem. Engin. Jap. **31**, 771 (1998).
[26] Y. Lilach and M. Asscher, J. Chem. Phys. **117**, 6730 (2002).
[27] R. S. Smith, C. Huang, E. K. L. Wong, and B. D. Kay, Phys. Rev. Lett. **79**, 909 (1997).
[28] J. Klanova, P. Klan, D. Heger, and I. Holoubek, Photochem. Photobiol. **2**, 1023 (2003).